THE UNIVERSITY OF TOKYO

Research Center for the Early Universe

RESCEU-29/97
UTAP-266/97

Cosmological Implications of Number Counts of Clusters of Galaxies: log$N$–log$S$ in X-Ray and Submm Bands

Tetsu KITAYAMA,[1] Shin SASAKI,[2] and Yasushi SUTO[1,3]

[1] *Department of Physics, The University of Tokyo, Tokyo 113*
E-mail(TK): kitayama@utaphp2.phys.s.u-tokyo.ac.jp
[2] *Department of Physics, Tokyo Metropolitan University, Hachioji, Tokyo 192-03*
[3] *Research Center for the Early Universe, School of Science, The University of Tokyo, Tokyo 113*

ABSTRACT

We compute the number counts of clusters of galaxies, the log$N$–log$S$ relation, in several X-ray and submm bands on the basis of the Press–Schechter theory. We pay particular attention to a set of theoretical models which well reproduce the *ROSAT* 0.5-2 keV band log$N$–log$S$, and explore possibilities to further constrain the models from future observations with *ASCA* and/or at submm bands. The latter is closely related to the European *PLANCK* mission and the Japanese Large Millimeter and Submillimeter Array (*LMSA*) project. We exhibit that one can break the degeneracy in an acceptable parameter region on the $\Omega_0 - \sigma_8$ plane by combining the *ROSAT* log$N$–log$S$ and the submm number counts. Models which reproduce the *ROSAT* band log$N$–log$S$ will have $N(>S) \sim (150-300)(S/10^{-12}\mathrm{erg\ cm^{-2}\ s^{-1}})^{-1.3}\ \mathrm{str}^{-1}$ at $S \gtrsim 10^{-12}\mathrm{erg\ cm^{-2}\ s^{-1}}$ in the *ASCA* 2-10 keV band, and $N(>S_\nu) \sim (10^2-10^4)(S_\nu/100\mathrm{mJy})^{-1.5}\ \mathrm{str}^{-1}$ at $S_\nu \gtrsim 100$mJy in the submm (0.85mm) band. The amplitude of the log$N$–log$S$ is very sensitive to the model parameters in the submm band. We also compute the redshift evolution of the cluster number counts and compare with that of the X-ray brightest Abell-type clusters. The results, although still preliminary, point to low density ($\Omega_0 \sim 0.3$) universes. The contribution of clusters to the X-ray and submm background radiations is shown to be insignificant in any model compatible with the *ROSAT* log$N$–log$S$.

Subject headings: Cosmology — Galaxies : clusters of — Radio sources : extended — X-rays : sources

Publications of the Astronomical Society of Japan, in press

1. Introduction

Clusters of galaxies are among the largest virialized structures in the universe and their importance as a cosmological probe is well-recognized. Thus their observations have been actively carried out in a variety of wavelengths including X-ray, optical, infrared, and radio bands. In the present paper, we focus on the theoretical predictions for the number counts of clusters of galaxies, the log$N$–log$S$ relation, rather than more conventional statistics such as the X-ray temperature and luminosity functions (hereafter XTF and XLF) for several reasons; 1) temperature of X-ray clusters can be reliably determined only for luminous ones, and thus the statistics is inevitably limited, 2) such obtained XTF is to some extent weighted towards relatively rich clusters, and may be biased for the luminous species, 3) the XTF and XLF at high redshifts ($z \gtrsim 0.1$) are in fact model-dependent statistics, because the translation of the observed X-ray flux to the absolute luminosity, and of the observed number to the comoving number density can be done only by assuming specific values of the cosmological parameters (the density parameter, Ω_0, the dimensionless cosmological constant, λ_0, and the Hubble constant H_0 in units of 100 km/s/Mpc, h).

On the other hand, the log$N$–log$S$ relation is almost free from the above problems as long as the cluster identification (or separation from point-like sources) and the conversion of count rates to fluxes are reliable. Recent analysis of the *ROSAT* Deep Cluster Survey (RDCS, Rosati et al. 1995, 1997) and the *ROSAT* Brightest Cluster Sample (BCS, Ebeling et al. 1997a,b) has determined the log$N$–log$S$ of clusters over almost four orders of magnitude in flux, i.e. $S(0.5\text{-}2.0 \text{ keV}) \sim 10^{-14} - 10^{-10}$ erg cm^{-2} s^{-1}. The number of identified clusters in the log$N$–log$S$ is over 200, an order of magnitude larger than that for the commonly used XTF based on Henry & Arnaud (1991), and therefore the log$N$–log$S$ data are statistically more reliable.

Kitayama & Suto (1997, hereafter KS97) found that a set of cold dark matter (CDM) models reproduce the above *ROSAT* log$N$–log$S$ data remarkably well over whole observed flux range, and simultaneously agree with the observed XTF and the *COBE* 4 year data. Nevertheless, there still exist some degeneracy of acceptable cosmological parameters. In the present paper, we explore possibilities to further constrain the models so as to break such degeneracy and discuss their implications in the following manner.

First, we combine the log$N$–log$S$ relations at different wavelengths, in X-ray and submm bands. The latter is of particular significance in relation to the future projects including the European *PLANCK* mission and the Japanese Large Millimeter and Submillimeter Array (*LMSA*) project. The emissions from intracluster gas in X-ray and submm bands are originated from completely different physical mechanisms; the former is mainly due to thermal bremsstrahlung, and the latter is due to the inverse-Compton scattering of the cosmic microwave background (CMB) photons, i.e. the Sunyaev & Zel'dovich (1972, hereafter SZ) effect. As a result, the log$N$–log$S$ relations in these bands show very different parameter dependence. We note that the submm log$N$–log$S$ was computed earlier by several authors (e.g., Barbosa et al. 1996;

Colafrancesco et al. 1997). Our analysis below differs from theirs in considering several CDM models consistent with the *ROSAT* log$N$–log$S$ data, in including the relativistic correction to the SZ effect, and in making quantitative and extensive predictions for the number counts on the $\Omega_0 - \sigma_8$ plane.

Second, we consider the cluster number counts incorporating redshift and/or temperature information in addition to the flux. In this way, we are able to discuss the evolution of cluster abundances on the basis of a cosmological model-independent and bias-free observable at high redshifts, which is in contrast to the approaches based on the XTF or XLF. We demonstrate a tentative comparison of our predictions with an observed sample from the *ROSAT* All Sky Survey, the X-ray brightest Abell-type clusters (Ebeling et al. 1996).

Finally, we discuss the implications of our results for the X-ray background (XRB) and the submm background radiation (SBR). Since the log$N$–log$S$ relation is closely related to the background radiation in the corresponding energy band, we may rigorously constrain the contribution of clusters of galaxies to the XRB and SBR.

2. Number counts of clusters of galaxies in X-ray and submm bands

2.1. X-ray flux from clusters

Following KS97, we compute the number of clusters observed per unit solid angle with X-ray flux greater than S by

$$N(>S) = \int_0^\infty dz\ d_A^2(z)\, c \left|\frac{dt}{dz}\right| \int_S^\infty dS\ (1+z)^3 n_M(M,z) \frac{dM}{dT_{\rm gas}} \frac{dT_{\rm gas}}{dL_{\rm band}} \frac{dL_{\rm band}}{dS}, \tag{1}$$

where c is the speed of light, t is the cosmic time, d_A is the angular diameter distance, $T_{\rm gas}$ and $L_{\rm band}$ are respectively the gas temperature and the band-limited absolute luminosity of clusters, and $n_M(M,z)dM$ is the comoving number density of virialized clusters of mass $M \sim M + dM$ at redshift z.

Given the observed flux S in an X-ray energy band $[E_a,E_b]$, the source luminosity $L_{\rm band}$ at z in the corresponding band $[E_a(1+z),E_b(1+z)]$ is written as

$$L_{\rm band}[E_a(1+z), E_b(1+z)] = 4\pi {d_L}^2(z) S[E_a, E_b], \tag{2}$$

where $d_L = (1+z)^2 d_A$ is the luminosity distance. Since the X-ray luminosity of clusters of galaxies depends sensitively on the details of the cluster gas density properties (distribution and clumpiness), its theoretical prediction as a function of M or $T_{\rm gas}$ is difficult. In fact, a simple self-similar model predicts for the bolometric luminosity, $L_{\rm bol} \propto T_{\rm gas}^2$, which is inconsistent with the observed relation $L_{\rm bol} \propto T_{\rm gas}^{3\sim3.5}$. Although a preheated cluster model might account for the latter (Kaiser 1991; Evrard & Henry 1991; Bower 1997), such theoretical models have not yet been

specified. Thus we adopt the observed $L_{\rm bol} - T_{\rm gas}$ relation parameterized by

$$L_{\rm bol} = L_{44} \left(\frac{T_{\rm gas}}{6{\rm keV}} \right)^{\alpha} (1+z)^{\zeta} \ \ 10^{44} h^{-2} \ {\rm erg \ sec^{-1}}. \tag{3}$$

As in KS97, we take $L_{44} = 2.9$, $\alpha = 3.4$ and $\zeta = 0$ as a fiducial set of parameters on the basis of recent observational indications (David et al. 1993; Ebeling et al. 1996; Ponman et al. 1996; Mushotzky & Scharf 1997). Then we translate $L_{\rm bol}(T_{\rm gas})$ into the band-limited luminosity $L_{\rm band}[T_{\rm gas}, E_1, E_2]$ as

$$L_{\rm band}[T_{\rm gas}, E_a(1+z), E_b(1+z)] = L_{\rm bol}(T_{\rm gas}) \times f[T_{\rm gas}, E_a(1+z), E_b(1+z)], \tag{4}$$

where $f[T_{\rm gas}, E_1, E_2]$ is the band correction factor which takes account of metal line emissions (Masai 1984) in addition to the thermal bremsstrahlung; the former makes significant contribution to the soft band luminosity especially at low temperature. Throughout this paper, we fix the abundance of intracluster gas as 0.3 times the solar value. Equations (2), (3) and (4) relate S and $T_{\rm gas}$ through $L_{\rm band}$, and are used to compute equation (1).

Assuming that the intracluster gas is isothermal, its temperature $T_{\rm gas}$ is related to the total mass M by

$$\begin{aligned} k_B T_{\rm gas} &= \gamma \frac{\mu m_p G M}{3 r_{\rm vir}(M, z_f)}, \\ &= 5.2 \gamma (1+z_f) \left(\frac{\Delta_{\rm vir}}{18\pi^2} \right)^{1/3} \left(\frac{M}{10^{15} h^{-1} M_\odot} \right)^{2/3} \Omega_0^{1/3} \ {\rm keV}. \end{aligned} \tag{5}$$

where k_B is the Boltzmann constant, G is the gravitational constant, m_p is the proton mass, μ is the mean molecular weight (we adopt $\mu = 0.59$), and γ is a fudge factor of order unity which may be calibrated from hydrodynamical simulations or observations. The virial radius $r_{\rm vir}(M, z_f)$ of a cluster of mass M virialized at z_f is computed from $\Delta_{\rm vir}$, the ratio of the mean cluster density to the mean density of the universe at that epoch. We evaluate this quantity using the formulae for the spherical collapse model presented in Kitayama & Suto (1996b) and assuming for simplicity that z_f is equal to the epoch z at which the cluster is observed.

Finally, we compute the mass function $n_M(M, z)dM$ in equation (1) using the Press–Schechter theory (Press & Schechter 1974) assuming $z = z_f$ as above. The effect of $z_f \neq z$ is discussed by KS97 in this context, and the more general consideration of $z_f \neq z$ is given in Lacey & Cole (1993), Sasaki (1994), and Kitayama & Suto (1996a,b).

2.2. Submm flux from clusters due to the Sunyaev-Zel'dovich effect

The inverse-Compton scattering of the CMB photons due to high temperature electron gas leads to distortion of the CMB spectrum (Sunyaev & Zel'dovich 1972). If the electrons are

non-relativistic, the change in the CMB intensity observed at frequency ν_0 at a position angle $\vec{\theta}$ from the cluster center is given by

$$\Delta I_\nu^{\rm NR}(x,\vec{\theta}) = \frac{2(k_B T_{\rm CMB})^3}{(h_{\rm P}c)^2} g(x) y(\vec{\theta}), \tag{6}$$

$$g(x) = \frac{x^4 e^x}{(e^x-1)^2}\left(x\coth\frac{x}{2}-4\right), \tag{7}$$

$$y(\vec{\theta}) = \int_{-\infty}^{\infty} \frac{k_B T_{\rm gas}(z)}{m_{\rm e}c^2}\sigma_{\rm T} n_{\rm e}(\vec{\theta},l) dl, \tag{8}$$

where $x \equiv h_{\rm P}\nu_0/(k_B T_{\rm CMB,0})$, $T_{\rm CMB,0} = 2.726$K is the present-day CMB temperature, $h_{\rm P}$ is the Planck constant, $\sigma_{\rm T}$ is the Thomson cross section, $m_{\rm e}$ is the electron mass, and $n_{\rm e}$ is the electron number density. At frequencies $\nu_0 > 217$GHz (or wavelengths < 1.4mm), $g(x)$ becomes positive and galaxy clusters become positive sources. In what follows we consider mainly the submm band at the observed wavelength 0.85mm ($\nu_0 = 350$GHz) where the emission from clusters is fairly strong ($x = 6.2$ and $g(x) = 6.7$) and the ground observations are feasible.

Then the total flux from a cluster located at redshift z is

$$\begin{aligned} S_\nu^{\rm NR}(x,M,z) &= \int \Delta I_\nu^{\rm NR}(x,\vec{\theta}) d^2\theta \\ &= 25.5\, h\,(1+z)\, g(x)\, \frac{1+X}{2}\frac{\Omega_{\rm B}}{\Omega_0^{2/3}}\left[\frac{d_A(z)}{cH_0^{-1}}\right]^{-2}\left(\frac{\Delta_{\rm vir}}{18\pi^2}\right)^{1/3}\left(\frac{M}{10^{15}h^{-1}M_\odot}\right)^{5/3}{\rm mJy}, \end{aligned} \tag{9}$$

where X is the hydrogen mass fraction for which we adopt $X = 0.76$ hereafter, and $\Omega_{\rm B}$ is the baryon density parameter (we adopt $\Omega_{\rm B} = 0.0125h^{-2}$). It should be noted that the above flux corresponds to the value averaged over the entire cluster, and the observed log$N$–log$S$ might be somewhat different depending on the details of the instruments specifically used in the survey. Aghanim et al. (1997) address this issue in detail.

At $T_{\rm gas} \gtrsim 10$ keV, the electrons become relativistic and the above expressions need to be modified. We thus apply the relativistic correction to equation (6) derived by Rephaeli (1995; see also Rephaeli & Yankovitch 1997). At 0.85mm, this leads to 4%, 11% and 16% reduction in flux at $T = 3$keV, 8keV and 12keV, respectively. We find that the relativistic correction at this wavelength is well fitted by

$$\Delta I_\nu^{\rm R} = \left[1 - 0.013\left(\frac{T_{\rm gas}}{1{\rm keV}}\right)\right]\Delta I_\nu^{\rm NR} \qquad \text{at 0.85mm.} \tag{10}$$

While clusters with $T_{\rm gas} \gtrsim 10$keV are rare and the above correction does not make significant difference, we take it into account for completeness in computing submm luminosity functions and the log$N$–log$S$. Since the above submm flux after the relativistic correction is explicitly expressed as a function of M and z, the submm log$N$–log$S$ is computed in a similar manner to equation (1).

3. Number counts in X-ray and submm bands predicted in the cold dark matter models

KS97 shows that CDM models with a certain range of parameters reproduce the *ROSAT* log$N$–log$S$ data as well as the XTF (Henry & Arnaud 1991) and the *COBE* 4 year data (Bunn & White 1997). To be definite, we hereafter consider five models with different sets of parameters summarized in table 1, and see if one can break the degeneracy of the models by comparing the log$N$–log$S$ relations in different bands. Throughout this paper, we assume that the primordial spectral index n is equal to unity and use the fitting formulae given in Kitayama & Suto (1996b) for the CDM mass fluctuation spectrum on the basis of Bardeen et al. (1986) transfer function.

Figure 1 shows the log$N$–log$S$ of clusters of galaxies in the soft X-ray (0.5-2 keV), hard X-ray (2-10 keV), and submm (0.85mm) bands. In the soft X-ray band, all the adopted models by definition reproduce well the observed log$N$–log$S$ from the *ROSAT* Deep Cluster Survey (RDCS, Rosati et al. 1995, 1997) and the *ROSAT* Brightest Cluster Sample (BCS, Ebeling et al. 1997a,b). In the hard X-ray band, massive clusters make slightly larger contribution to the predicted log$N$–log$S$ than in the soft band, and thus the lower Ω_0 models with flatter fluctuation spectra (i.e., more power at large scales) yield greater log$N$–log$S$. All the models are shown to lie under the upper limit inferred from the number of all X-ray sources observed by *ASCA* at 2-10 keV (Cagnoni et al. 1997), and they (except E1) are also consistent with the number of clusters observed by *HEAO 1* (Piccinotti et al. 1982) within the 1σ errors. The predicted count in model E1 is smaller than the *HEAO 1* result at the 3σ level (possible incompleteness in the *HEAO 1* result would simply raise the observed data point and does not reconcile the discrepancy).

In the submm band, on the other hand, the contribution from distant clusters becomes larger than in the X-ray bands (eqs [2]–[5] and [9]). Thus the lower Ω_0 models with slower evolution of fluctuations (i.e., more clusters at high z) yield greater log$N$–log$S$ as seen in figure 1(c). Compared with the hard X-ray band, the degeneracy of the models are broken in much greater extent in the submm band. Therefore, future determination of the submm cluster counts will enable us to constrain the models more tightly.

To see this clearly, we plot in figure 2 the contour maps of the cluster log$N$–log$S$ in different bands on the $\Omega_0 - \sigma_8$ plane. For the 0.5-2 keV band, the $1-\sigma$ significance level derived from the χ^2 test between our theoretical prediction and the observations (see KS97 for detail) is plotted, while for the 2-10 keV and submm bands, the contours of the number of clusters per steradian (10^2, 10^3, 10^4 from bottom to top) at S(2-10 keV) $= 10^{-13}$ erg cm^{-2} s^{-1}and $S_\nu(0.85\mathrm{mm}) = 10^2$mJy are plotted respectively. The σ_8 values derived from the *COBE* 4 year data (Bunn & White 1997) is also shown for reference. Panels (a) and (b) show that the contours for the 2-10 keV band counts run almost parallel to the χ^2 contour of the 0.5-2 keV band counts. In this sense, the future *ASCA* log$N$–log$S$ data will provide an independent consistency check of the *ROSAT* data. The shape of the submm log$N$–log$S$ contours, on the other hand, is quite different, especially at high σ_8, and thus should place complementary constraints on Ω_0 and σ_8.

In the conventional CDM power spectrum we have adopted, the spectral shape vary sensitively with Ω_0, h and $\Omega_{\rm B}$ through the shape parameter $\Gamma = \Omega_0 h \exp(-\Omega_{\rm B} - \sqrt{2h}\Omega_{\rm B}/\Omega_0)$ (Sugiyama 1995). In order to segregate the effects of changing the spectral shape, we further consider in the lower panels of figure 2 the 'CDM-like' spectrum with the fixed shape parameter $\Gamma = 0.25$ inferred from the galaxy correlation function (e.g., Peacock 1996) independent of Ω_0, h and $\Omega_{\rm B}$. The corresponding log$N$–log$S$ contours are similar to the conventional CDM case except at $\Omega_0 \lesssim 0.2$ and $\Omega_0 \gtrsim 0.8$, while the *COBE* normalized σ_8 is very sensitive to the changes in the spectral shape.

4. Evolution of cluster abundances

The evolutionary behavior of the cluster abundance would provide a useful probe of the cosmological parameters as discussed by a number of authors (e.g., Viana & Liddle 1996; Eke, Cole, Frenk 1996; Oukbir & Blanchard 1997; Mathiesen & Evrard 1997). It is of particular importance because the current and near future observations will provide us with the rapidly increasing amount of information on high redshift clusters. Thus we consider the evolution of cluster distribution and discuss whether one can break the degeneracy among the models inferred from the soft X-ray log$N$–log$S$ relation (table 1).

Figure 3 exhibits the redshift evolution of the number of clusters in different bands. As expected, the evolutionary behavior strongly depends on the values of Ω_0 and σ_8; the fraction of low redshift clusters becomes larger for greater Ω_0 and smaller σ_8. It is indicated that one may be able to distinguish among these models merely by determining the redshifts of clusters up to $z \sim 0.2$ (see also discussion below).

In order to characterize the physical properties of galaxy clusters, we have so far focused on their flux, because it is the simplest quantity which can be determined primarily from observations. Another major quantity of clusters is their temperature. Although the sample of clusters with measured temperature is still limited, an increasing amount of temperature information is going to become available from the *ASCA* (and future) observations. Furthermore, the temperature has an advantage in that it is insensitive to the detailed distribution of intracluster gas and much easier to model, compared to the X-ray flux or luminosity. This is in fact the main reason why many of the previous analysis of cluster abundance and its evolution are based upon the temperature rather than the X-ray luminosity (White, Efstathiou & Frenk 1993; Viana & Liddle 1996; Eke et al. 1996). However, the observed samples of clusters are usually flux limited, which needs to be kept in mind when one compares the theoretical predictions with the observed statistics. In our present framework, it is possible to incorporate explicitly the effects of limiting fluxes in the analysis based upon the cluster temperature.

Figure 4 shows the cumulative distribution of clusters with temperature greater than T, redshift less than z, and with/without the X-ray flux limit. It is apparent that the presence of a flux limit affects significantly the temperature distribution and its evolution, especially at low

T and high z. If the flux limit is $S = 10^{-12}$ erg cm^{-2} s^{-1}in the 0.5-2 keV band, for instance, the number of clusters observed with $T > 2$keV and $z < 0.3$ per unit solid angle is an order of magnitude less than what would have been expected without any flux limit.

The above discussion has clarified that the redshift evolution (at low z) and the temperature distribution of a given cluster sample with a specific flux limit can provide a useful probe of cosmological models. Unfortunately, we do not yet have a complete X-ray cluster sample with redshift and temperature information. However, one may still demonstrate the power of this approach using currently available 'best' sample. For this purpose, we adopt tentatively the X-ray brightest Abell-type clusters (XBACs, Ebeling et al. 1996), which is about 80 % complete and consists of 242 clusters with $S > 5 \times 10^{-12}$ erg cm^{-2} s^{-1}in the 0.1-2.4 keV band and $z < 0.2$. We use the temperature and redshift data compiled in table 3 of Ebeling et al. (1996). About 92 % and 30 % of all the clusters listed in this table have measured redshift and temperature, respectively. For the rest of the sample, the table also provides the redshifts estimated from the magnitude of the 10th-ranked cluster galaxy, and the temperatures estimated from the empirical $L - T$ relation. Keeping in mind the incompleteness of the sample and uncertainties especially in the estimated temperature data, we simply intend to perform a crude comparison with our predictions.

The results are plotted in figure 5. The sky coverage of the XBACs is hard to quantify mainly due to the uncertain volume incompleteness of the underlying optical catalogue as noted by Ebeling et al. (1996). In figure 5, therefore, we simply plot the real numbers of the XBACs and normalize all our model predictions to match the total number of the XBACs at its flux limit S(0.1-2.4 keV) $= 5 \times 10^{-12}$ erg cm^{-2} s^{-1}and redshift limit $z = 0.2$. In general, the model predictions are shown to be capable of reproducing well the shape and amplitude of the observed distributions $N(> S, > T, < z)$ even when T and z are varied. Taking into account the incompleteness of the observed data and large statistical fluctuations at low numbers, the agreements with models L03 and L03γ (both has $\Omega_0 = 0.3$) are rather remarkable. Since the shapes and amplitudes of the predicted curves in these figures are primarily determined by the value of Ω_0, this result provides a further indication for low Ω_0 universe.

5. Contribution to the X-ray and submm background radiation

The currently observed X-ray log$N$–log$S$ especially at faint flux end (Rosati et al. 1997; Rosati & Della Ceca 1997) places a model-independent constraint on the cluster contribution to the soft XRB. From the observed log$N$–log$S$ relation in figure 1(a), the cluster contribution to the XRB is estimated roughly as

$$I^{\rm cl}(0.5\text{-}2\ {\rm keV}) = \int_{S_{\rm min}}^{\infty} S \left| \frac{dN}{dS} \right| dS$$
$$\sim 2 \times 10^{-10} \left(\ln \frac{S_{12}}{S_{\rm min}} + 4.3 \right)\ {\rm erg\,cm^{-2}\,s^{-1}str^{-1}}, \qquad (11)$$

where $S_{12} \equiv 10^{-12}$ erg cm^{-2} s^{-1}, and we have fitted the 0.5-2 keV log$N$–log$S$ by a broken power-law: $N(>S) \propto S^{-1}$ at $S > S_{12}$ and $N(>S) \propto S^{-1.3}$ at $S < S_{12}$. The above estimate depends only weakly on the faint end flux $S_{\rm min}$, and taking for instance $S_{\rm min} = 10^{-15}$ erg cm^{-2} s^{-1}yields $I_{\rm cl}$(0.5-2 keV) $\sim 2 \times 10^{-9}$erg cm^{-2} s^{-1}str^{-1}, which is less than 10 % of the observed XRB (Gendreau et al. 1995; Suto et al. 1996).

To be more specific, we also compute numerically the contribution of clusters to the XRB. The XRB intensity $I_\nu^{\rm cl}(E_0)$ from clusters at energy E_0, as seen by an observer at present, is given by

$$I_\nu^{\rm cl}(E_0) = \frac{c}{4\pi H_0} \int_0^\infty dz \frac{J_\nu[E_0(1+z), z]}{(1+z)\sqrt{\Omega_0(1+z)^3 - K(1+z)^2 + \lambda_0}}, \tag{12}$$

where $J_\nu(E, z)$ is the comoving space-averaged volume emissivity at redshift z. We estimate this quantity by

$$J_\nu(E, z) = \int_0^\infty L_\nu(E, M, z)\, n_M(M, z)\, dM, \tag{13}$$

where the luminosity $L_\nu(E, M, z)$ of a cluster of mass M at z is computed in a similar manner to Section 2.1. It should be noted that the observed XRB spectrum is not derived from all sky surveys (in particular, at lower energy band), but from small regions in the sky where there are very few known bright X-ray sources. In order to compare with such observations, therefore, we also need to omit bright sources in our theoretical predictions by equation (12). For this purpose, we only consider contributions from clusters with flux below the critical value $S_{\rm crit}$(0.5-2 keV) $= 10^{-13}$ erg cm^{-2} s^{-1}, which roughly corresponds to the flux of the brightest X-ray source observed in the Lockman Hole by *ROSAT* (Hasinger et al. 1993).

Figure 6a exhibits the XRB intensity from clusters of galaxies in the cases of models L03 and E1, both of which reproduce the observed log$N$–log$S$ relation in the soft X-ray (0.5-2 keV) band. In these models, clusters contribute to the XRB only less than 20 % at $E_0 \lesssim 2$keV, which is consistent with the rough estimate described above. Thus, clusters of galaxies cannot be the major sources for the XRB even in soft X-ray bands (Evrard & Henry 1991; Oukbir, Bartlett, Blanchard 1997). As is clear from the above analysis, this conclusion is based on the observed log$N$–log$S$ relation, and almost independent of the assumed cosmological parameters. In fact, if one adopts a theoretical $L_{\rm bol} - T$ relation inferred from the self-similar assumption (Kaiser 1986) which yields $\alpha = 2$ in equation (3), there exist some models in which clusters account for the entire soft XRB (Blanchard et al. 1992; Kitayama & Suto 1996a). Such models, however, are simply in conflict with both the observed $L_{\rm bol} - T$ relation ($\alpha = 3 \sim 3.5$) and the *ROSAT* log$N$–log$S$.

A similar analysis can be performed for the SBR. Since we do not yet have the observed log$N$–log$S$ in the submm band, we fit the predicted log$N$–log$S$ of model L03 and obtain

$$\nu I_\nu^{\rm cl}(0.85{\rm mm}) \sim 10^{-12} \left(\frac{S_{\nu,{\rm min}}}{100{\rm mJy}}\right)^{-0.5} {\rm W\ m^{-2}\ str^{-1}}, \tag{14}$$

where we have assumed a single power law with $N(>S_\nu) \propto S_\nu^{-1.5}$. Taking $S_{\nu,{\rm min}} = 1$mJy gives $\nu I_\nu^{cl}(0.85{\rm mm}) \sim 10^{-11}$W m^{-2} str^{-1}, which is about 3% of the detected SBR by Puget et al.

(1996). Results from the numerical integration shown in figure 6b confirm that the clusters of galaxies contribute only less than $\sim 5\%$ of the SBR.

6. Conclusions

We have presented several cosmological implications of the number counts of clusters of galaxies. We have paid particular attention to the theoretical models which are in good agreement with the *ROSAT* log$N$–log$S$ in the soft X-ray (0.5-2 keV) band, and explored possibilities to further constrain the models from future observations in the *ASCA* hard X-ray and submm bands.

In the submm band (0.85mm), models which reproduce the *ROSAT* log$N$–log$S$ predict $N(>S_\nu) \sim (10^2 - 10^4)(S_\nu/100\mathrm{mJy})^{-1.5}$ str^{-1} at $S_\nu \gtrsim 100$mJy. We have shown that the amplitude of the above relation depend sensitively on Ω_0 and σ_8, and in a substantially different manner from the *ROSAT* log$N$–log$S$. Thus, combining the two can break the degeneracy in the acceptable parameter region on the $\Omega_0 - \sigma_8$ plane. This indicates that the future observations by the European *PLANCK* mission and the Japanese *LMSA* project would provide powerful probes of these parameters.

In the 2-10 keV band, the number counts show similar parameter dependence to those in the *ROSAT* 0.5-2 keV band, and we predict $N(>S) \sim 200(S/10^{-12}\mathrm{erg\,cm^{-2}\,s^{-1}})^{-1.3}$ str^{-1} at $S \gtrsim 10^{-12}\mathrm{erg\,cm^{-2}\,s^{-1}}$in the *ASCA* 2-10 keV band. The *ASCA* log$N$–log$S$ would therefore provide an important cross-check for our interpretation of the *ROSAT* log$N$–log$S$ data.

The evolutionary behavior of the number counts is also important to put additional cosmological constraints. We have exhibited that, given a complete flux limited cluster sample with redshift and/or temperature information, one can further constrain the cosmological models. We have performed a tentative comparison between our theoretical predictions and the recent compilation of the XBACs by Ebeling et al. (1996), which is the largest sample of galaxy clusters available to date. While the incompleteness of the sample and uncertainties in the temperature data still make it difficult to draw any definite conclusions from this comparison, it is interesting to note that our predictions reproduce well the evolutionary features of the XBACs and that the results, although preliminary, seem to favor low density ($\Omega_0 \sim 0.3$) universes.

The cluster log$N$–log$S$ also provides a tight constraint on their contribution to the background radiation in the corresponding energy band. Based on the log$N$–log$S$ relation observed by *ROSAT* in the 0.5-2 keV band, we conclude that clusters of galaxies contribute at most $\sim 20\%$ of the total XRB and less than $\sim 5\%$ of the SBR.

We are grateful to H. Ebeling and P. Rosati for generously providing us their X-ray data and helpful comments, and to K. Masai for making his X-ray code available to us. We also thank

A. Blanchard for valuable discussions, Y. Rephaeli for useful correspondences on the SZ effect, and the referee G. Zamorani for constructive comments. T.K. acknowledges support from a JSPS (Japan Society for the Promotion of Science) fellowship (09-7408). This research was supported in part by the Grants-in-Aid for the Center-of-Excellence (COE) Research of the Ministry of Education, Science, Sports and Culture of Japan (07CE2002) to RESCEU (Research Center for the Early Universe).

References

Aghanim, A., De Luca, A., Bouchet, F.R., Gispert, R., Puget, J.L. 1997, astro-ph/9705092

Barber, C. R., Roberts, T. P., Warwick, R. S. 1996, MNRAS 282, 157

Barbosa, D., Bartlett, J. G., Blanchard, A., Oukbir, J. 1996, A&A 314, 13

Bardeen, J. M., Bond, J. R., Kaiser, N., Szalay, A. 1986, ApJ 304, 15

Blanchard, A., Wachter, K., Evrard, A.E., Silk, J. 1992, ApJ 391, 1

Bower, R. G. 1997, astro-ph/9701014

Bunn, E. F., White, M. 1997, ApJ 480, 6

Cagnoni, I., Della Ceca, R., Maccacaro, T. 1997, astro-ph/9709018

Colafrancesco, S., Mazzotta, P., Rephaeli, Y., Vittorio, N. 1997, ApJ 479, 1

David, L. P., Slyz, A., Jones, C., Forman, W., Vrtilek, S. D. 1993, ApJ 412, 479

Ebeling, H., Voges, W., Böhringer, H., Edge, A. C., Huchra, J. P., Briel, U. G. 1996, MNRAS 281, 799

Ebeling, H., Edge, A. C., Fabian, A.C., Allen, S. W., Crawford C. S. 1997a, ApJ 479, L101

Ebeling H., et al. 1997b, MNRAS submitted

Eke, V. R., Cole, S., Frenk, C. S. 1996, MNRAS 282, 263

Evrard, A.E., Henry, J. P. 1991, ApJ 383, 95

Gendreau, K.C. et al. 1995, PASJ 47, L5

Hasinger, G. 1992, in The X-ray Background, eds. Barcons, X., Fabian, A. C. (Cambridge U.P.: Cambridge), 229

Hasinger, G., Burg, R., Giacconi, R., Hartner, G., Schmidt, M., Trümper, J., Zamorani, G. 1993, A&A 275, 1

Henry, J. P., Arnaud, K. A. 1991, ApJ 372, 410

Kaiser N. 1986, MNRAS 222, 323

Kaiser N. 1991, ApJ 383, 104

Kitayama, T., Suto, Y. 1996a, MNRAS 280, 638

Kitayama, T., Suto, Y. 1996b, ApJ 469, 480

Kitayama, T., Suto, Y. 1997, ApJ 490, in press (KS97)

Lacey, C. G., Cole, S. 1993, MNRAS 262, 627

Masai, K. 1984, Ap&SS 98, 367

Mathiesen, B., Evrard, A. E. 1997, astro-ph/9703176

Mushotzky, R.F., Scharf, C. A. 1997, ApJ 482, L13

Oukbir, J., Blanchard, A. 1997, A&A 317, 10

Oukbir, J., Bartlett, J. G., Blanchard, A. 1997, A&A 320, 365

Peacock J. A. 1996, MNRAS 284, 885

Piccinotti, G., Mushotzky, R. F., Boldt, E. A., Holt, S. S., Marshall, F. E., Serlemitsos, P. J., Shafer, R. A. 1982, ApJ 253, 485

Ponman, T. J., Bourner, P. D. J., Ebeling, H., Böhringer, H. 1996, MNRAS 283, 690

Press, W. H., Schechter, P. 1974, ApJ 187, 425 (PS)

Puget, J.-L., Abergel, A., Bernard, J.-P., Boulanger, F., Burton, W. B., Désert, F.-X., Hartmann, D. 1996, A&A 308, L5

Rephaeli Y. 1995, ARA&A 33, 541

Rephaeli Y., Yankovitch, D. 1997, ApJ 481, L55

Rosati, P., Della Ceca, R., Burg R., Norman, C., Giacconi, R. 1995, ApJ 445, L11

Rosati, P., Della Ceca, R. 1997, in preparation

Rosati, P., Della Ceca, R., Norman, C., Giacconi, R. 1997, ApJL submitted

Sasaki, S. 1994, PASJ 46, 427

Suto, Y., Makishima, K., Ishisaki, Y., Ogasaka, Y. 1996, ApJ 461, L33

Sugiyama, N. 1995, ApJS 100, 281

Sunyaev R.A., Zel'dovich Ya.B. 1972, Commts. Astrophys. Space Phys. 4, 173

Viana, P. T. P., Liddle, A. R. 1996, MNRAS 281, 323

White, S. D. M., Efstathiou, G., Frenk, C. S. 1993, MNRAS 262, 1023

Table 1. CDM model parameters from the *ROSAT* X-ray log$N$–log$S$.

Model	Ω_0	λ_0	h	σ_8	α	γ
L03	0.3	0.7	0.7	1.04	3.4	1.2
O045	0.45	0	0.7	0.83	3.4	1.2
E1	1.0	0	0.5	0.56	3.4	1.2
L03γ	0.3	0.7	0.7	0.90	3.4	1.5
L01α	0.1	0.9	0.7	1.47	2.7	1.2

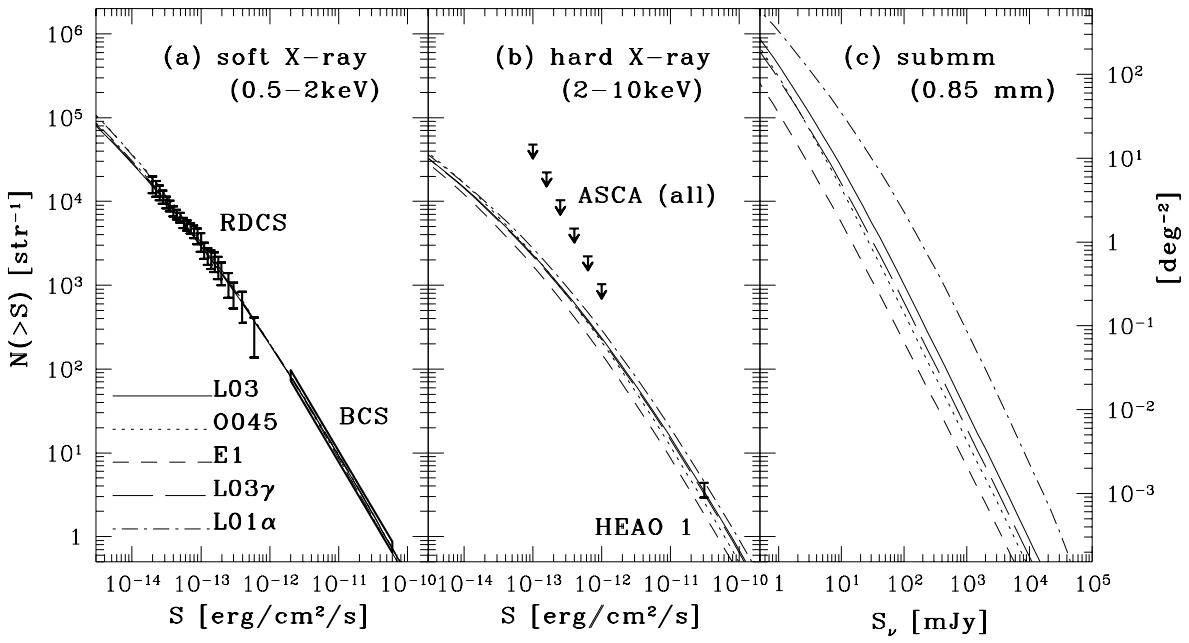

Fig. 1.— The log$N$–log$S$ relations of galaxy clusters for CDM models in (a) the soft X-ray (0.5-2.0 keV) band, (b) the hard X-ray (2-10 keV) band, and (c) the submm (0.85 mm) band. Lines represent the models listed in table 1; L03 (solid), O045 (dotted), E1 (short dashed), L03γ (long dashed), and L01α (dot-dashed). Also plotted in panel (a) are the 1σ error bars from the RDCS (Rosati et al. 1995, 1997), and the error box from the BCS (Ebeling et al. 1997a,b). In panel (b), the arrows indicate the log$N$–log$S$ of all X-ray sources in the 2-10 keV band from *ASCA* (Cagnoni et al. 1997), and the error bar (1 σ) is the number of clusters observed by *HEAO 1* (Piccinotti et al. 1982).

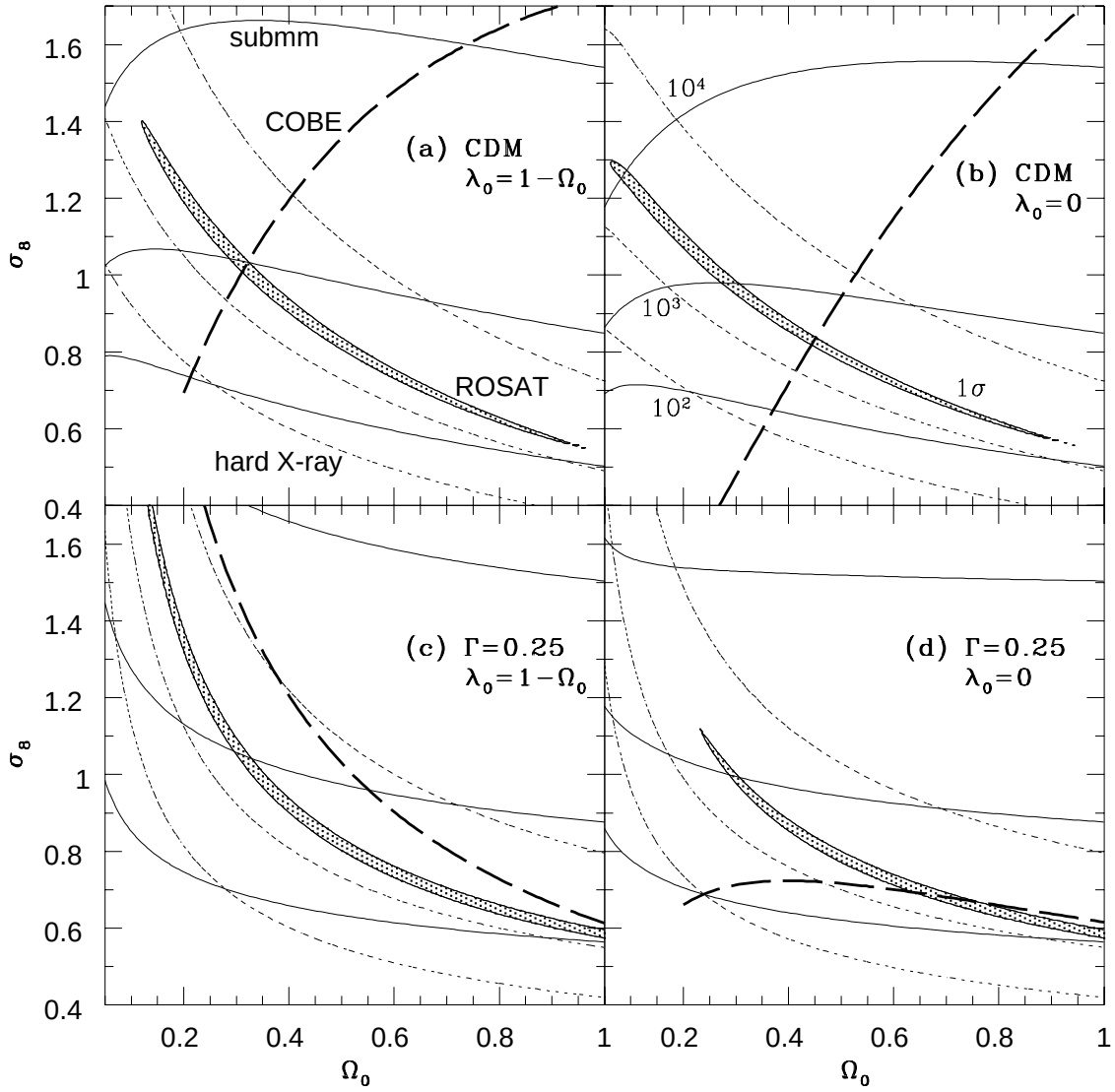

Fig. 2.— Contour maps on the Ω_0-σ_8 plane in (a) spatially flat ($\lambda_0 = 1 - \Omega_0$) CDM models, (b) open ($\lambda_0 = 0$) CDM models, (c) spatially flat CDM-like models with the fixed shape parameter ($\Gamma = 0.25$), and (d) open CDM-like models with $\Gamma = 0.25$. In all cases, $h = 0.7$, $\alpha = 3.4$, and $\gamma = 1.2$ are assumed. Shaded regions represent the 1σ significance contours derived in KS97 from the soft X-ray (0.5-2 keV) log$N$–log$S$. Dotted and solid lines indicate the contours of the number of clusters greater than S per steradian (10^2, 10^3, 10^4 from bottom to top) with $S = 10^{-13}$ erg cm^{-2} s^{-1}in the hard X-ray (2-10 keV) band and with $S_\nu = 10^2$mJy in the submm (0.85 mm) band, respectively. Thick dashed lines represent the *COBE* 4 year result computed from the fitting formulae at $0.2 < \Omega_0 \leq 1$ by Bunn & White (1997).

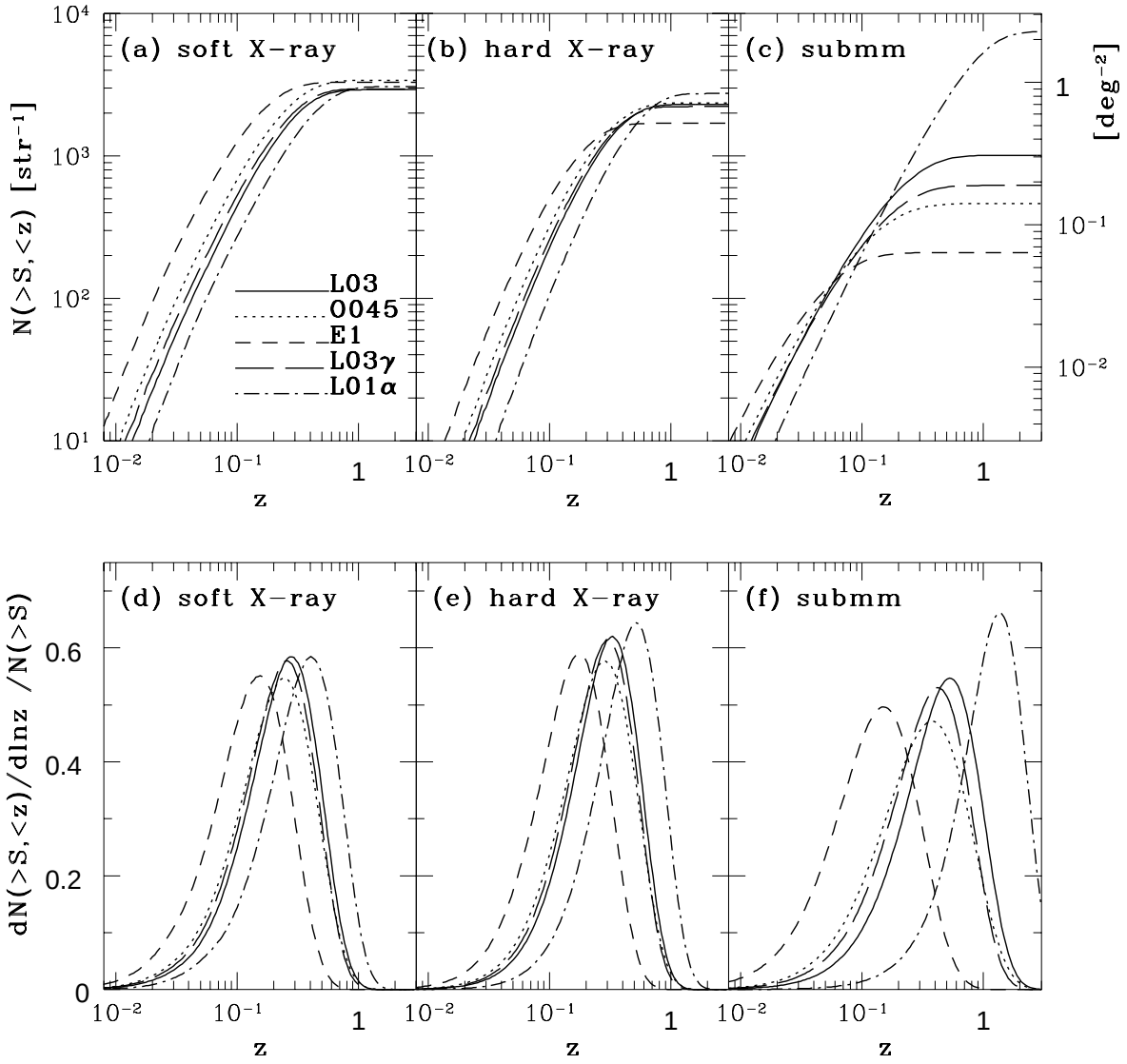

Fig. 3.— Redshift evolution of the number of galaxy clusters. Upper panels show the cumulative number $N(>S,<z)$ against z in (a) the soft X-ray (0.5-2 keV) band with $S = 10^{-13}$ erg cm^{-2} s^{-1}, (b) the hard X-ray (2-10 keV) band with $S = 10^{-13}$ erg cm^{-2} s^{-1}, and (c) the submm (0.85 mm) band with $S_\nu = 10^2$ mJy. Lower panels (d)–(f) are similar to (a)–(c) except for plotting the differential distribution $dN(>S,<z)/d\ln z$ normalized by $N(>S)$.

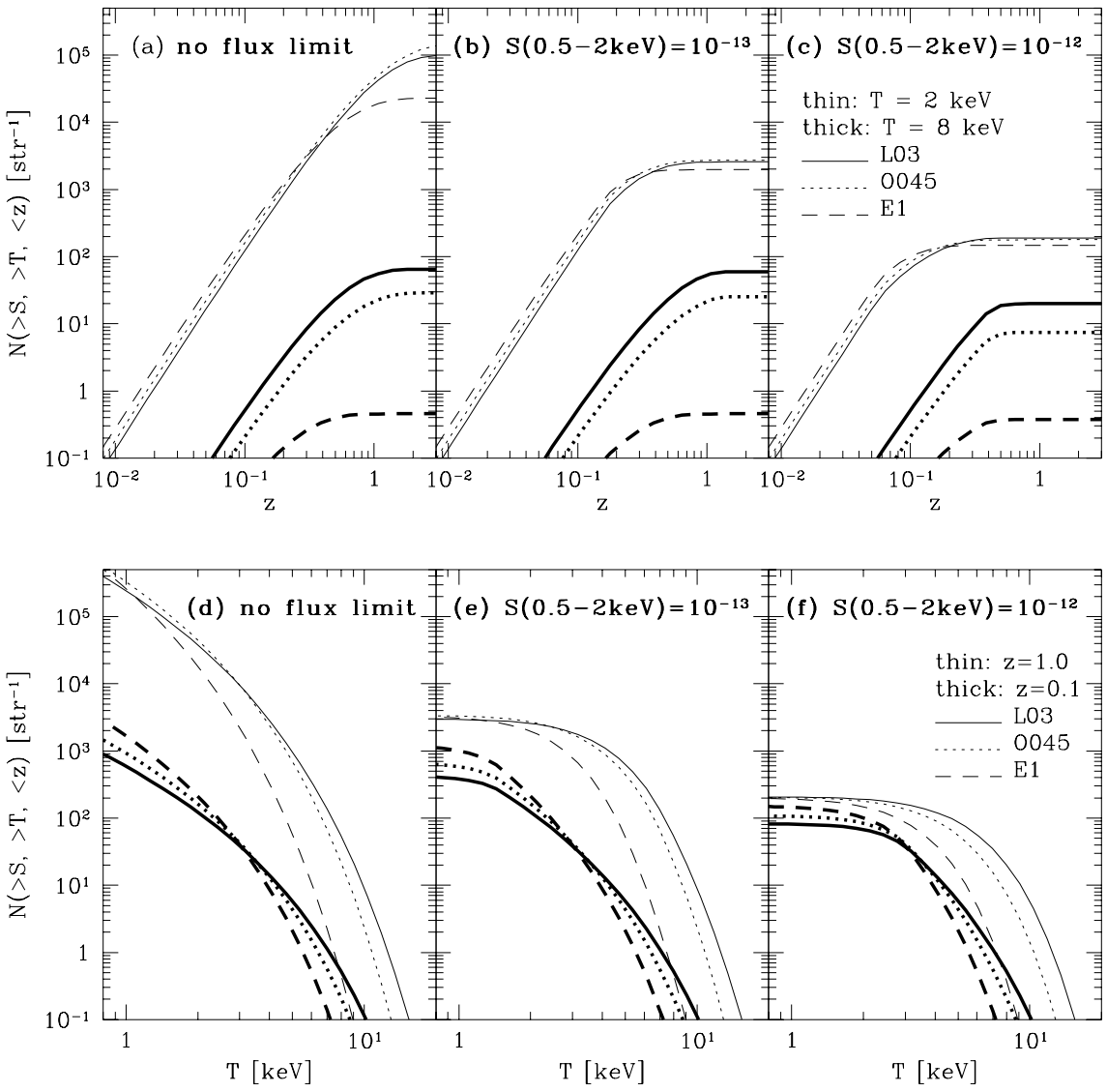

Fig. 4.— Effects of limiting fluxes on the redshift and temperature distributions of galaxy clusters. Upper panels exhibit the number $N(>S,>T,<z)$ against z for $T = 2$keV (thin lines) and $T = 8$keV (thick) in the cases of (a) $S = 0$ (no flux limit), (b) S(0.5-2keV) $= 10^{-13}$ erg cm^{-2} s^{-1}, and (c) S(0.5-2keV) $= 10^{-12}$ erg cm^{-2} s^{-1}. Lower panels (d)–(f) are similar to (a)–(c) except for plotting $N(>S,>T,<z)$ versus T in the cases of $z = 1$ (thin) and $z = 0.1$ (thick).

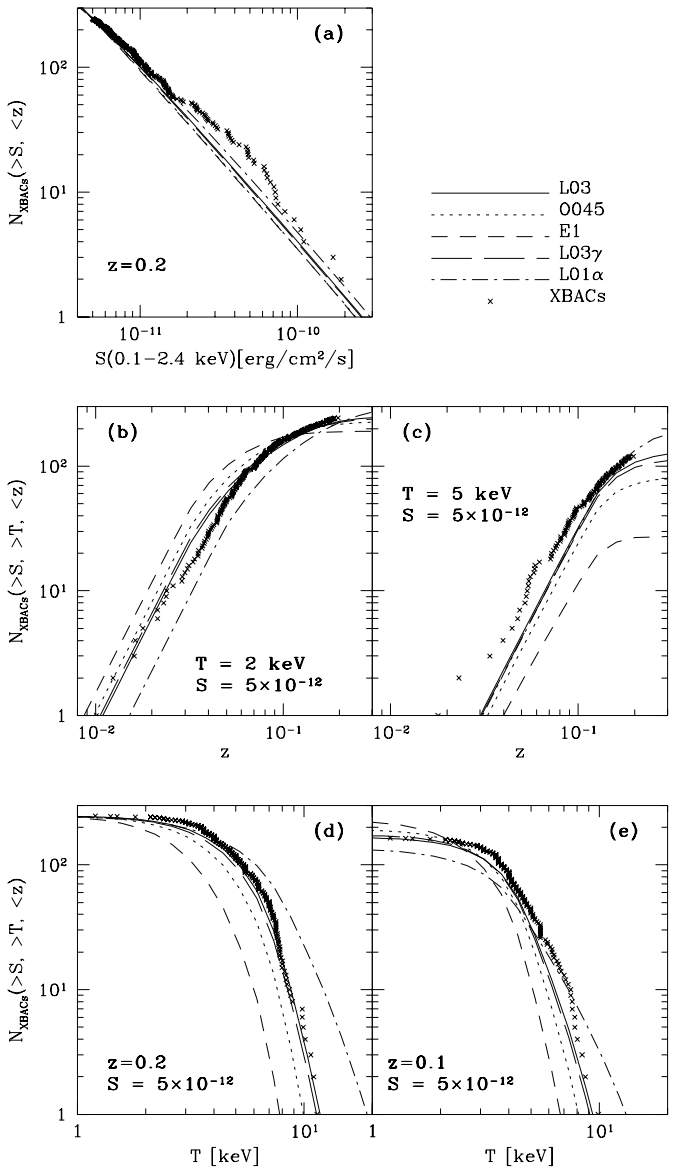

Fig. 5.— Tentative comparison with the XBACs (Ebeling et al. 1996). Upper panel (a) shows the log$N$–log$S$ in the 0.1-2.4 keV band with the redshift limit of $z = 0.2$ (models L03 and O045 almost overlap with L03γ and E1 respectively). Middle panels exhibit $N(>S, >T, <z)$ versus z for S(0.1-2.4 keV) $= 5 \times 10^{-12}$ erg cm^{-2} s^{-1}in the cases of (b) $T = 2$keV and (c) $T = 5$keV. Lower panels plot $N(>S, >T, <z)$ versus T for S(0.1-2.4 keV) $= 5 \times 10^{-12}$ erg cm^{-2} s^{-1}in the cases of (d) $z = 0.2$ and (e) $z = 0.1$. All the model predictions are normalized to reproduce the total number of the XBACs at its flux limit S(0.1-2.4 keV) $= 5 \times 10^{-12}$ erg cm^{-2} s^{-1}and redshift limit $z = 0.2$.

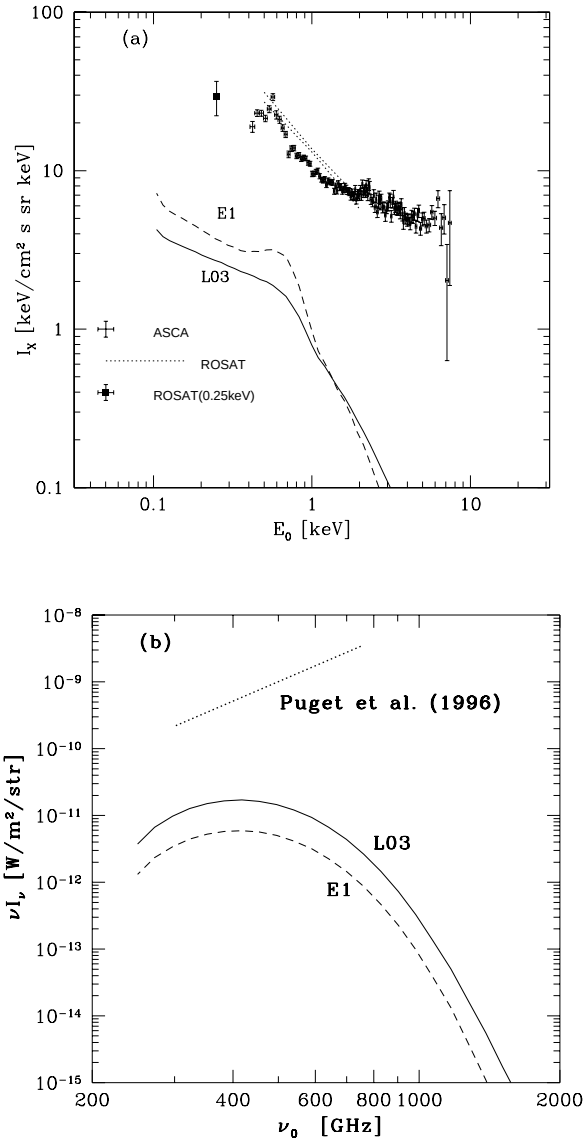

Fig. 6.— Contribution of clusters of galaxies to (a) the XRB, and (b) the SBR, in models L03 (solid) and E1 (dashed). Also shown are the observed XRB data of *ASCA* (Gendreau et al. 1995), *ROSAT* (Hasinger 1992), *ROSAT* at 0.25 keV (Barber et al. 1996), and the tentative detection of the cosmic far-infrared background by *COBE* (Puget et al. 1996).